ELSEVIER

Denitrification rates and excess nitrogen gas concentrations in the Arabian Sea oxygen deficient zone

A.H. Devol[a,*], A.G. Uhlenhopp[a], S.W.A. Naqvi[b], J.A. Brandes[c], D.A. Jayakumar[d], H. Naik[b], S. Gaurin[e], L.A. Codispoti[f], T. Yoshinari[g]

[a]School of Oceanography, University of Washington, Box 357940, Seattle, WA 98195, USA
[b]National Institute for Oceanography, Dona Paula, Goa 403 004, India
[c]Skidaway Institute of Oceanography, 10 Ocean Circle Drive, Savannah, GA 31411, USA
[d]Princeton University, Princeton, NJ 08544, USA
[e]Smith College, Northampton, MA 01063, USA
[f]Horn Point Laboratory, University of Maryland, Cambridge, MD 21613, USA
[g]New York State Department of Health and School of Public Health, SUNY, Albany, NY 12201-0509, USA

Abstract

Rates of canonical, i.e. heterotrophic, water-column denitrification were measured by ^{15}N incubation techniques at a number of coastal and open ocean stations in the Arabian Sea. Measurements of N_2:Ar gas ratios were also made to obtain independent estimates of N_2 excess resulting from denitrification. Measured denitrification rates ($^{15}NO_3^- \rightarrow ^{15-14}N_2$) at open ocean stations averaged $9.1 \pm 1.0\ nmol\ N\,l^{-1}\,d^{-1}$ ($n = 15$), and coastal rates averaged $33.2 \pm 12.4\ nmol\ N\,l^{-1}\,d^{-1}$ ($n = 18$). When extrapolated to the entire Arabian Sea, deep measurements within the offshore perennial suboxic zone indicate an overall denitrification rate of $41\ Tg\ N\,a^{-1} \pm 18\ Tg\ N\,a^{-1}$, which is within the range (10–$44\ Tg\ N\,a^{-1}$) of previous estimates for canonical denitrification in the region based on stoichiometric calculations and electron transport system activity. Nitrogen excess gas measurements predict a larger nitrogen anomaly than estimated by classical stoichiometric methods (maximum anomaly $= 23\ \mu g$ at $N\,l^{-1}$ vs. $13\ \mu g$ at $N\,l^{-1}$, respectively). This mismatch may result from incorrect assumptions of Redfield stoichiometry inherent in the nitrate deficit calculation, inputs of new nitrogen through N-fixation, N_2 contributions from sedimentary denitrification along continental margins, the anammox reaction, and metal catalyzed denitrification reactions. Nevertheless, if denitrification is defined as the conversion of combined nitrogen to a gaseous end product, then the data suggest that denitrification in the Arabian Sea may have been underestimated so far.
© 2006 Elsevier Ltd. All rights reserved.

*Corresponding author.

E-mail addresses: devol@u.washington.edu (A.H. Devol), uhopp@ocean.washington.edu (A.G. Uhlenhopp), naqvi@csnio.ren.nic.in (S.W.A. Naqvi), brandes@skio.peachnet.edu (J.A. Brandes), ajayakum@Princeton.edu (D.A. Jayakumar), naik@csnio.ren.nic.in (H. Naik), Gaurin@email.smith.edu (S. Gaurin), codispot@hpl.umces.edu (L.A. Codispoti), yoshinar@wadsworth.org (T. Yoshinari).

1. Introduction

Fixed nitrogen (NO_3^-, NO_2^-, NH_4^+, R-NH$_2$, etc.) has long been known to be an important biolimiting nutrient in vast areas of the world's oceans (Codispoti, 1989). As such, nitrogen is integrally linked to primary production and carbon cycling with its availability controlling not only the fertility

of the oceans but also the sequestration of carbon dioxide from the atmosphere. Despite its importance, some aspects of the marine nitrogen cycle are still not well understood. For example, whether or not the combined nitrogen budget in the present day ocean is balanced has been a topic of considerable debate (Codispoti and Christensen, 1985; Gruber and Sarmiento, 1997; Codispoti et al., 2001; Deutsch et al., 2001). Most recent studies suggest that the oceans are, on balance, losing fixed nitrogen, but the magnitude of the net loss is not well quantified (Codispoti et al., 2001).

Water-column and sedimentary denitrification are the two major sinks in the marine-combined nitrogen budget. (Here, we define denitrification as the conversion of fixed nitrogen to N_2 gas, i.e., canonical, or heterotrophic, denitrification, anammox, nitrifier denitrification, etc.) Current estimates of water column denitrification range from 60 to 250 Tg N a^{-1} (Codispoti, 1995; Middelburg et al., 1996; Gruber and Sarmiento, 1997). With the entire marine-combined nitrogen turnover rate in the neighborhood of 200–500 Tg N a^{-1}, a range of 190 Tg N a^{-1} in the water-column denitrification component is clearly significant. Water-column denitrification is thought to occur only in suboxic environments, overwhelmingly in oxygen deficient zones (ODZs) of the world's oceans (Codispoti et al., 2005). The Arabian Sea is one of the three ODZs (the other two being the eastern tropical North and South Pacific), contributing significantly to global water column denitrification (Naqvi, 1987; Naqvi and Shailaja, 1993; Codispoti et al., 2001).

Oxygen deficient conditions (defined as $O_2 \leqslant 0.1$ ml l^{-1} or $\sim 4\,\mu M$; Codispoti et al., 2005) in the Arabian Sea are the consequence of its unusual geographical setting, which greatly affects regional circulation and biological productivity (Naqvi et al., 2003; Morrison et al., 1999). Atmospheric and surface oceanic circulations in the northern Indian Ocean are governed by two distinctly opposite monsoon cycles that are known to produce some of the greatest seasonal variability of any ocean basin (Smith et al., 1998). During the southwest monsoon (June–August) strong winds blowing from the southwest produce offshore Ekman transport triggering intense coastal upwelling off Somalia, Yemen and Oman. The coastally upwelled water is transported hundreds of kilometers offshore, enriching the euphotic zone with nutrients (Morrison et al., 1999). This, in conjunction with high aeolian dust flux and near constant, intense irradiance,

results in high primary production (~ 1.5 g C m^{-2} d^{-1}; Barber et al., 2001, Lee et al., 1998). The northeast monsoon (December–February) is characterized by cold, dry winds that blow from the northeast and cause convective mixing over a large area. The associated nutrient pumping sustains primary production (1–2 g C m^{-2} d^{-1}), which is comparable with that during the southwest monsoon (Barber et al., 2001). High primary productivity creates high O_2 demand at depth and is one major factor responsible for prevalence of suboxic conditions in the Arabian Sea.

The other primary element contributing to suboxic conditions is the restricted supply of O_2 to intermediate depths. The ODZ is supplied with water advecting in from three major areas: the southern Indian Ocean, the Persian Gulf and the Red Sea. The latter two sources have modest preformed O_2 concentrations, and also make relatively minor contributions to the water budget of the ODZ (Swallow, 1984). Most of the water responsible for renewal of the ODZ is derived from the southern Indian Ocean. This water outcrops around 40°S, and while its preformed O_2 concentration is high, the long trajectory of flow results in great reduction of the O_2 content by the time this water reaches the southern border of the ODZ ($\sim 12°$N) (Warren, 1994). Thus the O_2 supply does not keep pace with its consumption for the decay of copious organic matter sinking from the productive surface waters, thus producing the strong and persistent ODZ in the Arabian Sea.

Published estimates of water column denitrification in the Arabian Sea range from 0.1 to 44 Tg N a^{-1}; even if the lowest estimate (0.1 Tg N a^{-1} based on a seemingly high choice of renewal time—30 yr; Dueser et al., 1978) is ignored, the range of remaining estimates is still quite wide (10–44 Tg N a^{-1}; Naqvi, 1987; Mantoura et al., 1993; Naqvi and Shailaja, 1993; Howell et al., 1997; Codispoti et al., 2001). These estimates also assume canonical denitrification ($NO_3^- \rightarrow NO_2^- \rightarrow NO \rightarrow N_2O \rightarrow N_2$) to be the main process that converts fixed-N to gaseous N_2, but additional pathways such as the anammox reaction (e.g., Devol, 2003; Kuypers et al., 2003) are becoming increasingly recognized. Importantly, none of the published estimates are based on direct measurements; indeed, this applies equally well to estimates for the other ODZs. Most water-column denitrification rates are derived from stoichiometry-based calculations that are typically expressed as 'nitrogen

anomalies', a concept that allows the amount of nitrate removed from the water column to be quantified. Nitrogen anomalies are classically calculated from hydrographic data, and are routinely presented as nitrate deficits, i.e., as a pool of "missing" nitrate resulting from denitrification. These deficits are then combined with an estimate of the residence time of denitrifying waters in order to compute a denitrification rate. An alternate way to express nitrogen anomalies is as nitrogen gas (N_2) excess, i.e., the pool of "extra" N_2 resulting from denitrification. The amount of excess N_2 has not been measured directly in the Arabian Sea, with existing denitrification rates obtained largely using the nitrate deficits, so that uncertainties and assumptions inherent in the deficits are carried into the rates.

In this paper, we present profiles of the excess nitrogen gas concentration through the ODZ of the Arabian Sea as determined by measurement of N_2:Ar gas ratios. We also present denitrification rates estimated from the conversion of ^{15}N–NO_3^- to $^{29}N_2$ during in situ and shipboard incubations of water samples and discuss these in relation to canonical denitrification and anammox.

2. Methods

2.1. Study site

Samples were collected during six cruises in the Arabian Sea and the Indian Ocean, between 1994 and 1999 aboard the R.V. *Knorr* (WOCE leg I7N; Table 1 and Fig. 1), R.V. *Sagar Sampada* (SS141, SS161), and R.V. *Sagar Kana* (SK137, SK140, SK148)(Table 2, Fig. 1).

2.2. N_2:Ar profiles

N_2:Ar water column measurements were made on five of the six cruises at stations covering a wide latitudinal range in the western and central Arabian
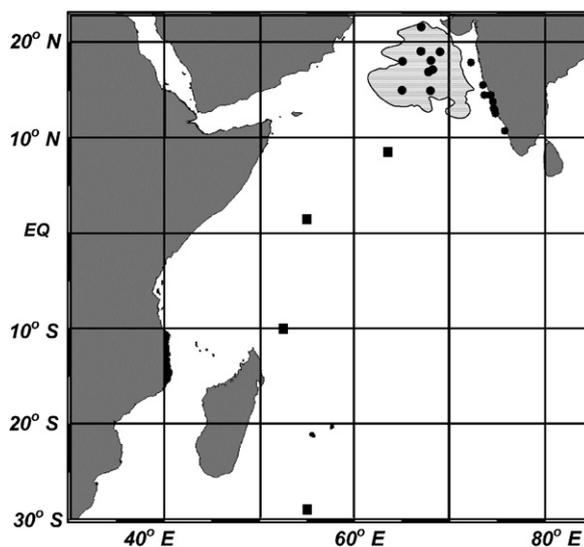

Fig. 1. Sampling locations. The shaded area represents the approximate area of the oxygen-deficient, denitrifying zone. Squares denote the 4 WOCE stations used as reference stations. See Table 1 for specific station locations.

Sea (Fig. 1) using the method described by Emerson et al. (1991) and Hamme and Emerson (2003). Samples were taken by siphoning approximately 125 ml of water from a Niskin bottle into a 250 ml evacuated glass sample container poisoned with 50 μl of saturated $HgCl_2$. The method includes stringent precautions to ensure the sample water was never in contact with the atmosphere. Samples were returned to the University of Washington where they were placed in a temperature-controlled water bath to equilibrate the dissolved gases with the headspace. After equilibration the liquid portion of the sample was removed and the remaining gas was cryogenically transferred into a stainless steel sample tube immersed in liquid He. After extraction, sample tubes were interfaced with a Finnegan MAT 251 isotope ratio mass spectrometer (IRMS) and analyzed for atomic masses 28, 29 and 40 according to the method described by Emerson et al. (1991) and Hamme and Emerson (2003).

2.3. ^{15}N incubations

Denitrification rates were determined by measuring the conversion of ^{15}N–NO_3^- to $^{29}N_2$ in incubated water samples. At the time these measurements were made (1996–99), canonical denitrification was thought to be the main process by which N_2 was produced in the oceans. For that reason, we measured only $^{29}N_2$. (With only canonical denitrification taking

Table 1
Station locations for WOCE stations outside the ODZ

Station name in text	Latitude	Longitude	WOCE Leg
28 S	28° 58.81′S	55° 00.45′E	I7
10 S	10° 07.22′S	52° 28.17′E	I7
1 S	1° 34.21′S	55° 00.0′E	I7
8 N	8° 30.77′N	63° 34.03′E	I7

Table 2
Station locations and measured denitrification rates for open ocean and coastal sites confidence limits are given for samples where 3 or more points are in the time series (standard error of the rate)

Cruise	Date	Latitude	Longitude	Depth (m)	Incubation type	Ambient $^{15}NO_3$ ($\mu mol\,l^{-1}$)	$^{15}NO_3$ added ($\mu mol\,l^{-1}$)		Rate ($nmol\,l^{-1}y^{-1}$)
Open ocean									
*SS161	Jan-98	19°N	67°E	300	In situ	21.7	5		8.2
*SS161	Jan-98	17°N	68°E	202	On deck	21.3	5		4.9±0.3
SS161	Jan-98	17°N	68°E	210	In situ	21.4	5		12.3
SS161	Jan-98	17°N	68°E	300	On deck	24.2	5		5.3±1.7
*SS161	Jan-98	18°N	65°E	290	On deck	22.4	5		7.0±2.8
SS161	Jan-98	18°N	65°E	290	In situ	22.4	5		3.7
SS161	Jan-98	17°N	68°E	278	In situ	24.2	5		11.9
SS141	Apr-96	15°N	65°E	300	In situ	22.1	5		15.0
SS141	Apr-96	19°N	67°E	300	In situ	22.1	5		11.9±2.3
SS141	Apr-96	19°N	69°E	250	In situ	25	5		8.5
*SK148	Sep-99	17°N	68°E	225	On deck	24.2	6		14.0
*SK148	Sep-99	18°N	68°E	200	On deck	23.8	6		8.6
*SK148	Sep-99	21.5°N	67°E	200	On deck	17.8	6		13.9
SK148	Sep-99	21.5°N	67°E	300	On deck	14.3	7.5		5.0
SS140	Dec-98	15°N	68°E	150	On deck	21.9	5		5.4
								Average	9.1±1.0
Coastal									
*SK137	Aug-98	10.7°N	75.8°E	23	On deck	15.8	7		7.6±1.1.63
*SK137	Aug-98	12.5°N	74.8°E	22	On deck	9.4	5		7.2
SK137	Aug-98	12.5°N	74.8°E	30	On deck	9.1	5		7.2
SK137	Aug-98	12.8°N	74.7°E	31	On deck	11.2	5		7.6±2.7
*SK137	Aug-98	13.1°N	74.6°E	32	On deck	4.8	5		13.4±0.4
*SK137	Aug-98	13.8°N	74.5°E	13.5	On deck	5.9	5		2.8±2.0
SK137	Aug-98	13.8°N	74.5°E	22	On deck	0.3	5		10.0±0.72
*SK137	Aug-98	14.5°N	74.3°E	20	On deck	4	5		13.2±1.3
SK137	Aug-98	14.5°N	74.2°E	21	On deck	13.7	5		5.4
SK137	Aug-98	14.5°N	74.2°E	30	On deck	14.4	5		15.9±9.53
*SK137	Aug-98	15.5°N	73.6°E	22	On deck	12.6	5		25±3.4
*SK148	Sep-99	12.9°N	74.7°E	28	On deck	12.5	5		68.3
SK148	Sep-99	14.5°N	74.2°E	27	On deck	11.4	5		126.9
*SK148	Sep-99	14.5°N	74.2°E	27	On deck	11.4	5		207±53
SK148	Sep-99	14.5°N	74.3°E	25	On deck	11.3	6		14.3
*SK148	Sep-99	15.5°N	73.5°E	30	On deck	19	6		26.6±5.5
SK148	Sep-99	17.9°N	72.2°E	72	On deck	10.5	6		25.8
SK148	Sep-99	17.9°N	72.2°E	72	On deck	10.5	6		11.4
								Average	33.2±12.4

Statistics on averages are standard errors. Stations marked with an * are plotted in Fig. 2.

place we could predict the amount of $^{30}N_2$ formed from the mole fractions of $^{14}NO_3^-$ and $^{15}NO_3^-$ in the incubations.) Thus, our denitrification measures do not directly include the production of N_2 by the anammox reaction nor can they rule out anammox as a pathway of $^{29}N_2$ production (see Section 4). ^{15}N incubations were conducted both in situ and on deck on five of the Arabian Sea cruises (SS141, SS161, SK137, SK140 and SK148) at both shallow (<35 m) coastal stations and deep, open-ocean stations (Fig. 1). For in situ incubations a spring powered

syringe containing a $^{15}N–NO_3^-$ solution (100 at%) in saturated NaCl solution (to facilitate quick dispersal of the labeled NO_3^-) was attached to the outside of a Niskin bottle. Nylon tubing (1/8 in i.d.) passing through a hole drilled in the air vent of the Niskin bottle connected the syringe with the upper part of the sampler, and a similar tubing extending from the lower part of the sampler vented outside near the top of the sampler (this was to allow the escape of excess water from inside the sampler once the syringe was fired). The syringe was held in the cocked position by

a lanyard attached to the Niskin tripping mechanism. At the appropriate depth the Niskin bottle was tripped and the syringe fired, releasing the ^{15}N–NO_3^- tracer into the bottle. The amount and concentration of tracer added was enough to increase the ambient NO_3^- concentration ($\sim$25 μM) by 5 μM. The bottle remained in the water at depth for the duration of the incubation, after which time it was brought to the surface and sampled. Samples were taken into the evacuated, poisoned glass sample containers and run on an IRMS as described above.

On deck incubations were carried out in 1-l amber glass bottles. Water was transferred into the bottles in such a way that it was never in contact with the atmosphere, thus maintaining suboxic conditions. Silicone stoppers containing two lengths of 1/8 in nylon tubing with valves were placed in the bottles. One of the pieces of tubing (for filling the bottle and drawing samples) extended to the bottom of the incubation bottle. The other piece of tubing (for water and air venting) extended only to the middle of the stopper. The long piece of tubing was then connected to the Niskin sample bottle containing water from the appropriate depth and the 1-l bottle was filled and overflowed by several volumes before the inlet valve was closed. The ^{15}N–NO_3^- was injected directly through the stopper with a needle long enough to reach the bottom of the bottle while the vent valve was open so that excess water could escape from the bottle. Incubations took place in a cold room within 3 °C of ambient temperatures for 10–30 h. At the conclusion of each incubation, samples were again taken into the evacuated, poisoned glass containers and run on the IRMS as previously described.

Denitrification rates were calculated from change in the 28/29 mass ratio during the incubation assuming canonical denitrification was the dominant N_2 production pathway. Given this assumption we can statistically predict the distribution of $^{28}N_2$, $^{29}N_2$ and $^{30}N_2$ during canonical denitrification based on the known mole fractions of $^{14}NO_3^-$ and $^{15}NO_3^-$ in the incubation. Departures from this assumption due to anammox are discussed in following sections. To calculate the concentrations of ^{14}N and ^{15}N in N_2 gas at the start of the incubation from the measured initial $\delta^{15}N_2$ we made the assumption that the N_2 concentration of the sample was the atmospheric equilibrium concentration at in situ temperature and salinity. This is not strictly true due to non-equilibrium effects (Hamme and Emerson, 2003) and N_2 additions due to

denitrification itself. However, these effects only change the equilibrium concentration by about 2% and result in only about a 5% change in the calculated rate. Given the above, the $^{15}N/^{14}N$ ratio of the N_2 gas at the end of the experiment is given by the expression:

$$\left(\frac{15}{14}N\right)_f = \frac{[^{15}N]_i + R\Delta T\left(\frac{15}{14}NO_3\right)}{[^{14}N]_i + R\Delta T\left\{1 - \frac{15}{14}(NO_3)\right\}}, \quad (1)$$

where $[^{15}N]_i$ and $[^{14}N]_i$ are the concentrations of ^{15}N and ^{14}N in the N_2 gas (ng-at l^{-1}) at the start of the incubation, R is the denitrification rate (nmol l^{-1} d^{-1}), ΔT is the incubation time (d) and $\left(\frac{15}{14}NO_3\right)$ is the ratio of isotopes in the nitrate pool. Solving Eq. (1) for R and correcting for the unmeasured $^{30}N_2$ that would also be formed during denitrification one obtains:

$$R = \frac{[^{15}N]_i + \left(\frac{15}{14}N\right)_f [^{14}N]_i}{\left[\left(\frac{15}{14}N\right)_f - \left(\frac{15}{14}N\right)_f \left(\frac{15}{14}NO_3\right) - \left(\frac{15}{14}NO_3\right)\right]\Delta T}$$

$$\times \left\{\frac{1}{1 - \left(\frac{15}{14}NO_3\right)^2}\right\}, \quad (2)$$

where the last term is the $^{30}N_2$ correction. This correction will be larger for larger mole fractions of $^{15}NO_3^-$. The correction results in only a minor change in the average pelagic rate, from 8.6 to 9.1 nM d^{-1} but a larger correction for the coastal data, 22–33 nM d^{-1}, because coastal nitrate concentrations were lower.

2.4. Nutrients

Oxygen, nutrients, and salinity were analyzed on deck within 3 h of sample collection. Dissolved oxygen was measured using the Winkler method. Nutrients were analyzed on a SKALAR 6-Channel Analyzer 5100/1 using standard methods (Grasshoff et al., 1983). Salinity was measured with a Guildline salinometer. Hydrographic data for the WOCE stations were obtained from the WOCE program office (http://whpo.ucsd.edu/).

3. Results

3.1. Oxygen and nitrate profiles

Oxygen and nitrate profiles measured at the open Arabian Sea stations were typical of the ODZ of the Arabian Sea (Fig. 2(a) and (b)). Oxygen concentrations were virtually zero from 150 to 800 m. Nitrate
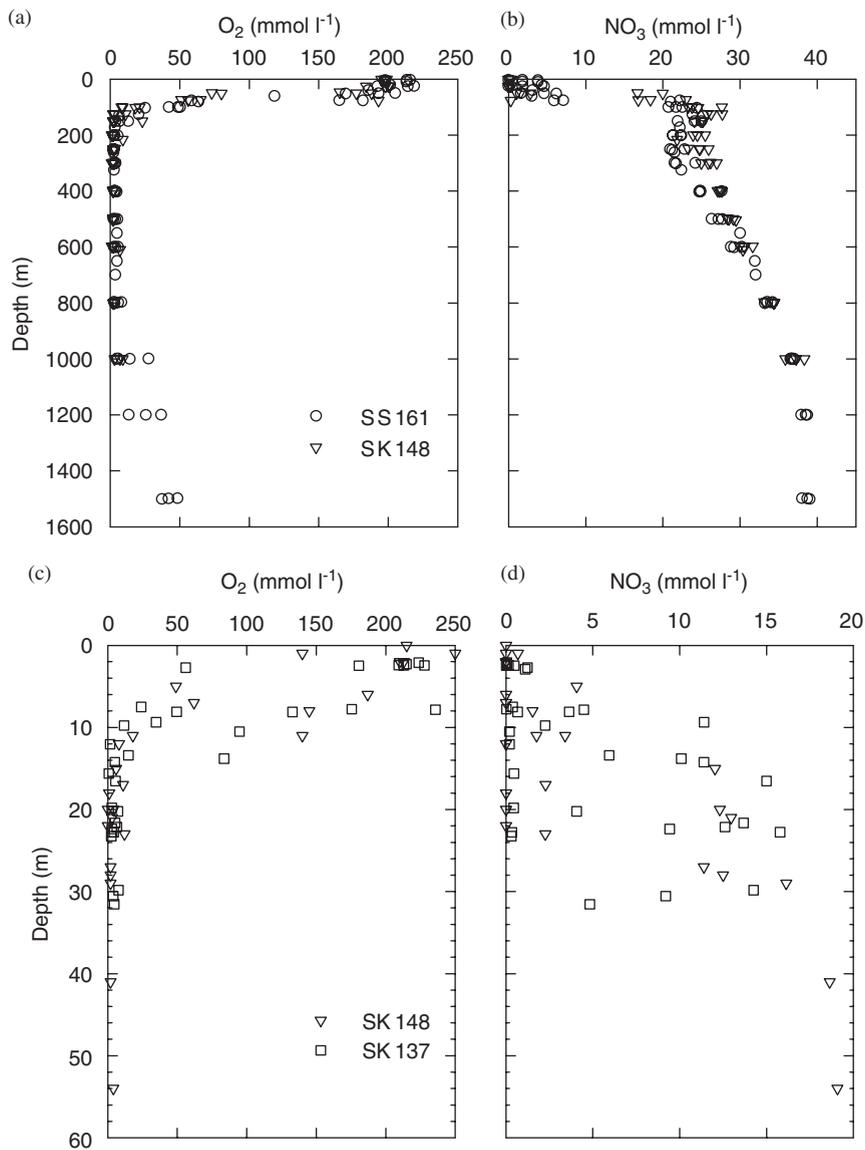
Fig. 2. Dissolved oxygen (a) and NO$_3$ (b); profiles from representative central Arabian Sea stations along with oxygen (c) and NO$_3$ (d) profiles from representative coastal stations. Stations plotted are marked with an * in Table 2.

concentrations were near zero at the surface, increased to approximately 25 μM at about 150 m, decreased slightly between 150–500 m, and asymptotically increased to ~40 μM from 500 to 1500 m. The dip in the nitrate profile around 200 m has been well documented in the past and is indicative of denitrifying conditions (Naqvi, 1987; Morrison et al., 1999).

The two cruises which covered the shelf were undertaken during the period of upwelling and O$_2$ deficiency in near-bottom waters (Naqvi et al., 2000). Accordingly, while the dissolved O$_2$ concen-

trations at the coastal stations were high at the surface (~200 μM), the O$_2$ content quickly decreased to zero by approximately 15–20 m. Nitrate concentrations were near zero at the surface and typically increased to 10–20 μM by ~15 m depth (Fig. 2(c) and (d)).

3.2. Denitrification rates

^{15}N–N$_2$ in the incubations increased from 0.5‰ to 1.0‰ over the course of most incubations (Fig. 3), which is well within the precision of the

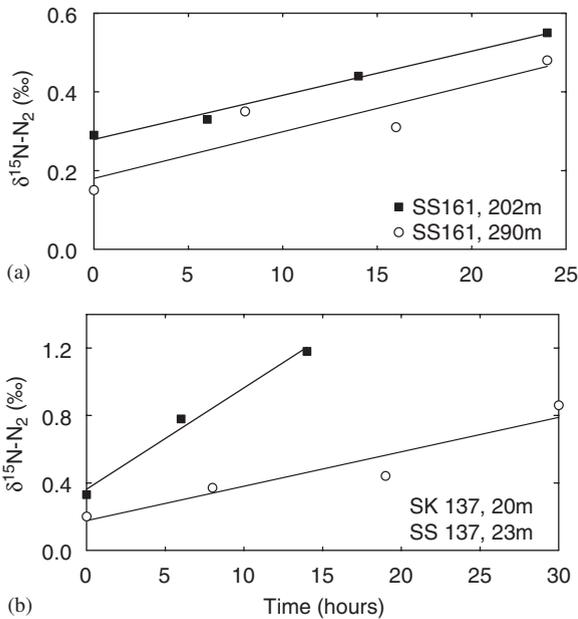Fig. 3. Representative change in $^{15}N–N_2$ (‰) over time in the ^{15}N-labeled incubations for open ocean (a) and coastal (b) incubations.
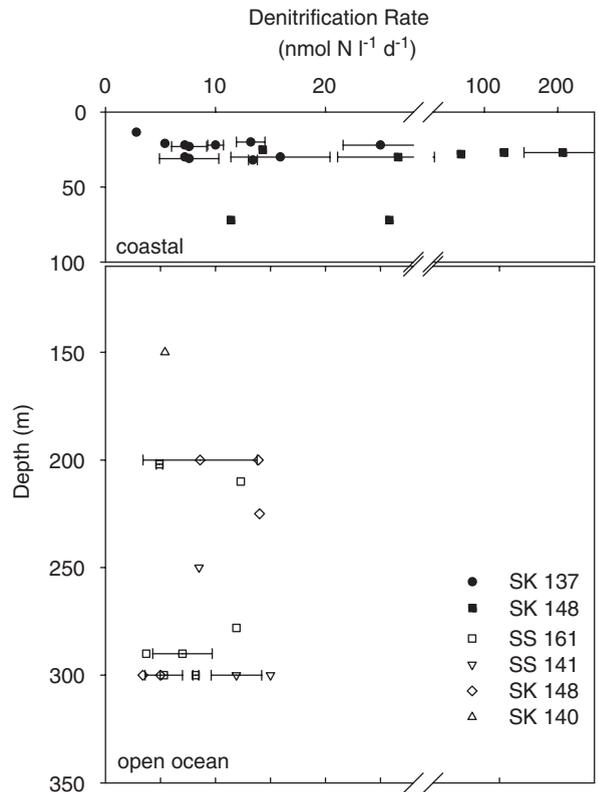

Fig. 4. Vertical profiles of measured denitrification rates (nmole $N l^{-1} d^{-1}$) at coastal (upper) and open ocean (lower) stations. Error bars represent standard errors in Table 2. *Note*: These are two separate composite profiles, not a single composite.

measurement of ± 0.5‰ based on 221 sample duplicates (175 from ALOHA and 46 from the Arabian Sea). Although most incubations included only initial and final time points, an adequate number (14 of 33 of incubations) included 3–4 time points and suggested $^{15}N–N_2$ production was quasi-linear. There were no significant differences between on deck and in situ incubations. Canonical denitrification rates for coastal waters varied widely, from 5 to 207 nmol $N l^{-1} d^{-1}$ with generally higher rates during SK148 than SK137. They were also, on average, higher than rates from the deep stations (Table 2, Fig. 4). Denitrification rates from deep stations ranged from 4.9 to 15 nmol $N l^{-1} d^{-1}$ (Table 2, Fig. 4). There were no apparent spatial differences in the measured rates, nor was there any discernible depth distribution (Fig. 4). However, given that there were only a few depths sampled from any given station, and that stations spanned a large geographic and temporal range, the lack of trends is not surprising. Since there were no large differences between the measured rates, especially in the open ocean, each set of data from the coastal and deep stations was averaged. Coastal denitrification rates averaged 33.2 ± 12.4 nmol $N l^{-1} d^{-1}$ and average deep rates were 9.0 ± 1.0 nmol $N l^{-1} d^{-1}$ (Table 2).

3.3. N_2 excess

Gas ratio data collected from source waters south of the Arabian Sea ODZ exhibited values consistent with oxic marine regions. Although there were large and systematic variations in the hydrographic variables from the four stations on the WOCE transect, (e.g., O_2, NO_2^-; Fig. 2), N_2:Ar values for these stations outside the ODZ did not differ appreciably (Fig. 5: N_2:Ar values have been divided by equilibrium saturation values (Emerson et al., 1999) to give normalized N_2:Ar ratios so that a value of 1.000 indicates equilibrium). Normalized N_2:Ar ratios were approximately 1.000 at the surface and increased with depth to about 1.014 by 2500 m. The solid line (Figs. 5(b) and 6) represents the best fit of the data from the 4 WOCE stations to sigma-t values (N_2:Ar $= -1.5976 + 0.3263\sigma_t - 0.01365\sigma_t^2 + 0.000191\sigma_t^3$). These data from the Indian Ocean are very similar to all other N_2:Ar profiles that have been measured outside ODZs (Fig. 5(b)) including the North Pacific
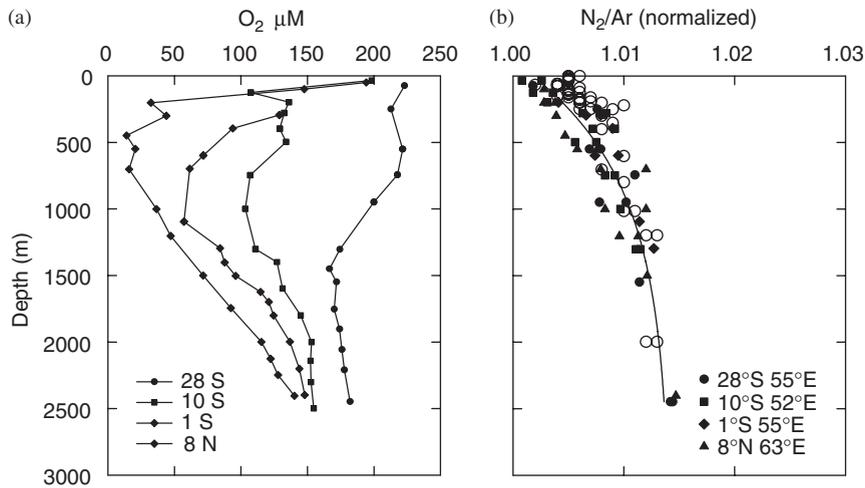
Fig. 5. (a) Dissolved oxygen versus depth for the 4 Indian Ocean WOCE stations (Table 1); (b) normalized N2:Ar ratios for the the 4 WOCE stations (solid symbols along with data from station ALOHA (HOT data: open symbols). The line represents the polynomial fit to the WOCE data referred to in the text.
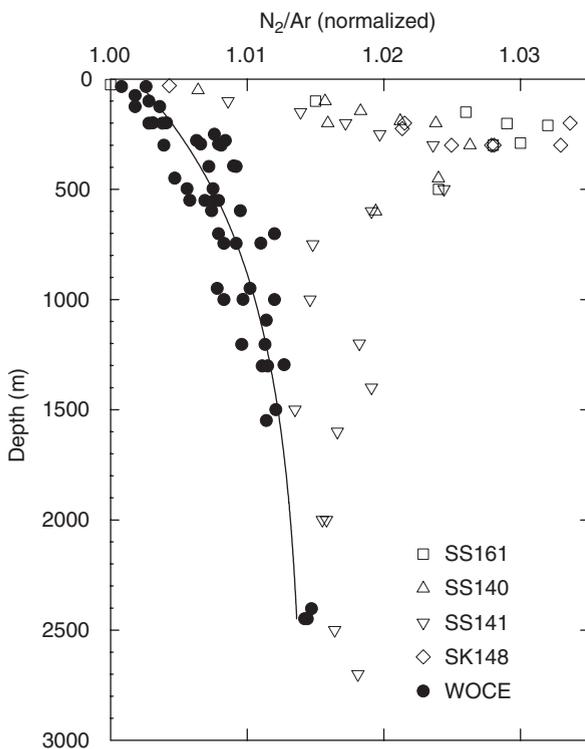

Fig. 6. Normalized N_2:Ar ratios for the ODZ stations in the Arabian sea along with ratios for the WOCE data.

subtropical gyre (Station ALOHA, Hamme, 2003; also plotted on Fig. 5(b)), Washington and California margins (Hartnett, personal communication), and the Southern Ocean (Uhlenhopp, unpublished data). Although these gas ratios seem to indicate

supersaturation of N_2 outside the ODZ, recent work by Hamme (2003) suggests the gases are not supersaturated, but rather slightly undersaturated with N_2 less undersaturated than Ar. This is due to bubble injection and differential non-equilibrium conditions during water mass formation. Since the trend of increasing normalized ratios with depth appears to be widespread and consistent through the Pacific, Indian and Southern Oceans, we will assume this profile is the normal oceanic background, and that data from the WOCE stations accurately represent water entering the ODZ of the Arabian Sea.

In contrast, N_2:Ar profiles inside the denitrifying zone were strikingly different. Although the surface values were once again near 1.00, there was a distinct peak in the heart of the ODZ at about 200–300 m where values reached 1.030–1.035 (Fig. 6). From this peak values decreased until they returned to values typical of the WOCE stations outside of the ODZ at about 1500 m.

4. Discussion

Denitrification rates presented in Table 2 are for canonical denitrification based on the assumption that it was the dominant process of N_2 production during the incubation. However, given the recent discovery of anammox in marine systems (Dalsgaard and Thamdrup, 2002) and in the oxygen minimum zone waters of the Benguela upwelling system (Kuypers et al., 2003), this assumption may not be

entirely valid. If anammox is occurring in the Arabian Sea ODZ, which, as we discuss below, seems likely, then our rates of N_2 production are underestimates of the true rate. Also, at the extreme, if anammox were the sole production pathway of N_2 in the Arabian Sea and if denitrifiers were only reducing nitrate to nitrite, then if the denitrification was in isotopic equilibrium with the ambient nitrite pool our rate estimates would be approximately correct. This is because in either process basically one labeled N combines with one unlabeled N to form $^{29}N_2$. However, it is unlikely that the NO_2^- pool would be in isotopic equilibrium and labeled NO_2^- would need to grow into the ambient NO_2^- pool. In this case, the odds of combining a labeled and unlabeled N would increase during the course of the incubation and our results would again be underestimates.

Measured denitrification rates were higher and much more variable at coastal stations (average = $33.2 \pm 12.4 \, \text{nmol N} \, l^{-1} \, d^{-1}$) than those at deep stations (average = $9.0 \pm 1.0 \, \text{nmol N} \, l^{-1} \, d^{-1}$; Table 2). Denitrification in near bottom waters over the Indian continental shelf occurs seasonally (during late summer and autumn), as a result of the combination of strong near-surface thermohaline stratification and high primary production. Although the latter is sustained primarily by nutrient supply through upwelling, there is reason to believe that increased fertilizer runoff from land might have led to an intensification of this process in recent years (Naqvi et al., 2000). During the periods of our observations, suboxic conditions were well developed in the region. Interestingly, conditions in the low oxygen waters over the Indian shelf are similar to those of the Benguela upwelling zone where anammox was shown to be the dominant N_2 production pathway (Kuypers et al., 2003).

Although the highest denitrification rate measured at the coastal stations ($188 \, \text{nmol N} \, l^{-1} \, d^{-1}$) is an order of magnitude higher than most other coastal rates, it is not unreasonably high. The water at the coastal stations is presumably upwelled from $\sim$100–125 m, so that its initial nitrate concentration would be $\sim$25 µM (Fig. 2; also see Niak, 2003). Observations indicate that nitrate concentrations are seasonally variable, and by September denitrification often leads to the complete removal of nitrate in the upwelled water over the inner shelf north of $\sim$12°N latitude (Niak, 2003). With the maximal observed denitrification rate, nitrate would be completely depleted in about 4 months, which is longer than the time actually taken ($<$2 months;

Niak, 2003) for the onset of sulfate reduction after the system turns suboxic (denitrifying). This indicates that, if anything, our estimates for coastal waters may be conservative.

Previous researchers estimated pelagic denitrification rates in the Arabian Sea by indirect methods, primarily through the use of nitrate deficits combined with varying choices of residence time for the ODZ water (Naqvi, 1987; Mantoura et al., 1993; Howell et al., 1997; Bange et al., 2000). The only non-nitrate deficit based observational estimate has come from the work of Naqvi and Shailaja (1993) who used enzymatic measurements of activity of electron transport system (ETS) to estimate denitrification rates. Additionally, there are two modeling-based estimates provided by Yakushev and Neretin (1997), and Kawamiya and Oschlies (2003). An advantage of these methods is that they provide estimates with adequate temporal and spatial coverage because they are based on routine hydrographic data. However, the primary disadvantage is that they compound uncertainties in the nitrate deficit calculation and the water mass residence time. An additional shortcoming is that neither the anomaly nor the rate has been measured, only calculated. In addition, as noted earlier, these methods assume that nitrate loss is only due to canonical denitrification or slight modifications of canonical denitrification.

In the majority of previous studies in the Arabian Sea (e.g., Naqvi and Sen Gupta, 1985; Mantoura et al., 1993; Bange et al., 2000) nitrate deficit has been computed using the semi-conservative water mass tracer 'NO' introduced by Broecker (1974). This property is defined as 'NO' = $[O_2] + 9.1[NO_3^-]$, with the factor 9.1 representing the Redfield ratio between O_2 consumption and NO_3^- regeneration. This approach usually involves establishment of a relationship between 'NO' and potential temperature for waters outside the denitrification zone. The solution of the 'NO' equation for NO_3^- yields the "expected NO_3^-", NO_3^{-exp}, within the denitrification zone from temperature and O_2 (Naqvi and Sen Gupta, 1985). The nitrate deficit is then simply the difference between NO_3^{-exp} and the measured $NO_3^- + NO_2^-$. Nitrate deficits are either integrated over the volume of the denitrification zone and combined with residence time or used in conjunction with estimates of water mass transport out of the denitrification zone to arrive at a denitrification rate. Recently, Codispoti et al. (2001) suggest that these NO-based methods underestimate the nitrate deficit (see below).

A common problem in comparing denitrification rate estimates based on depth integrated nitrate deficits is that different authors assume different residence times and surface areas of the denitrification zone in the Arabian Sea. Nevertheless, all recent denitrification rate estimates fall in the range of 13–34 Tg a^{-1} (Bange et al., 2000; Howell et al., 1997; Mantoura et al., 1993; Naqvi, 1987; Yakushev and Neretin, 1997). Naqvi and Shailaja (1993), used an enzymatic measurement of the activity of the ETS (Packard, 1971; Codispoti and Packard, 1980) to estimate a denitrification rate of 24–33 Tg a^{-1}. While this rate is independent of residence time, it is still dependent on the area of the denitrification zone (moreover, it also involves assumptions concerning the conversion of ETS activity to denitrification rate). When all estimates are normalized to a common denitrification area of 1.5×10^{12} m^2 (the average of Mantoura et al. (1993) and Naqvi (1987) areas) the range of estimates becomes 9.5 Tg a^{-1} (Mantoura et al., 1993) to 44 Tg a^{-1} (Naqvi and Shailaja, 1993) still varying over a factor of more than four.

Although we lack sufficient rate measurements to construct a comprehensive depth or seasonal structure in the Arabian Sea, the rates measured by us in the open ocean compare reasonably well to previous estimates of denitrification in the area. As a first approximation, we have multiplied the measured open ocean average rate by 600 m, a depth zone where oxygen deficiency is the most extreme and denitrification rates are likely at a maximum, to derive an areal average rate. Integrating this rate over the area of denitrifying waters in the Arabian Sea (1.5×10^{12} m^2) and assuming the rate remains constant throughout the year, the rate of denitrification in the Arabian Sea becomes 41 ± 18 Tg N a^{-1}, which falls within the range of previous estimates.

Our estimate of 41 Tg N a^{-1} does not include measurements from coastal stations. Since the coastal stations were typically < 50 m deep, and there is currently no precise estimate for the spatial extent of coastal denitrification, these rates cannot be extrapolated with confidence. Volumetric denitrification rates at the coastal stations are on average 3.6 times higher than deep rates (Table 2), indicating that the estimate of 41 Tg N a^{-1} for canonical denitrification in the entire Arabian Sea is probably conservative.

Our measured rates and those estimated from nitrate deficits should be directly comparable because they are both based solely on the removal of nitrate from the water column. However, since there are components of denitrification other than just the removal of nitrate, both sets of estimates are expected to be systematically lower than the actual values. The most obvious is the probable conversion of the ammonia (NH$_3$) remineralized during denitrification to N$_2$, likely by anammox type reactions (NH$_4^+$ + NO$_2^-$ → N$_2$ + 2H$_2$O, Dalsgaard and Tharmdrup, 2002; Jetten et al., 2003; Kuypers et al., 2003). If we define denitrification as the conversion of fixed nitrogen to N$_2$, this and other pathways leading to N$_2$ production must be included.

An alternate and independent method to assess the amount of denitrification is to directly measure the excess nitrogen gas in the water column. The final product of denitrification, N$_2$, has no other significant sources or sinks within interior water masses, and thus the amount of excess N$_2$ reflects the amount of denitrification. Measuring the nitrogen gas excess captures the N$_2$ produced not only from the reduction of NO$_3^-$, but also from the remineralization and denitrification of ammonia in organic matter (R-NH$_3$), as well as any other processes converting combined nitrogen to N$_2$.

The amount of excess N$_2$ gas in the Arabian Sea ODZ was estimated from our normalized N$_2$:Ar ratios as follows:

$$[N]_{excess} = [(N_2 : Ar)_{sample} - (N_2 : Ar)_{background}][N]_{(t,s)}, \tag{3}$$

where (N2:Ar)$_{sample}$ is the normalized ratio within the denitrifying waters of the ODZ (Fig. 6), (N$_2$:Ar)$_{background}$ is the normalized ratio predicted for a parcel of water outside the denitrifying zone with the same density (estimated from the best fit line through the WOCE background data, Fig. 5) and [N]$_{(t,s)}$ is the atmospheric equilibrium saturation of N$_2$ predicted from temperature and salinity data. Ar concentrations are assumed to be equal in both sample and background waters of equal density. We have chosen to express nitrogen concentrations in units of μg-at N, so that there is 1:1 relationship between NO$_3^-$–N denitrified and N$_2$–N excess.

An ensemble profile of excess N$_2$ within the denitrifying zone of the Arabian Sea is shown in Fig. 7. Excess N$_2$ is essentially zero in the surface waters but increases within the ODZ to a maximum of approximately 16–25 μg-at N around 250 m depth. The amount of excess N$_2$ decreases slowly thereafter; however, the values remain slightly
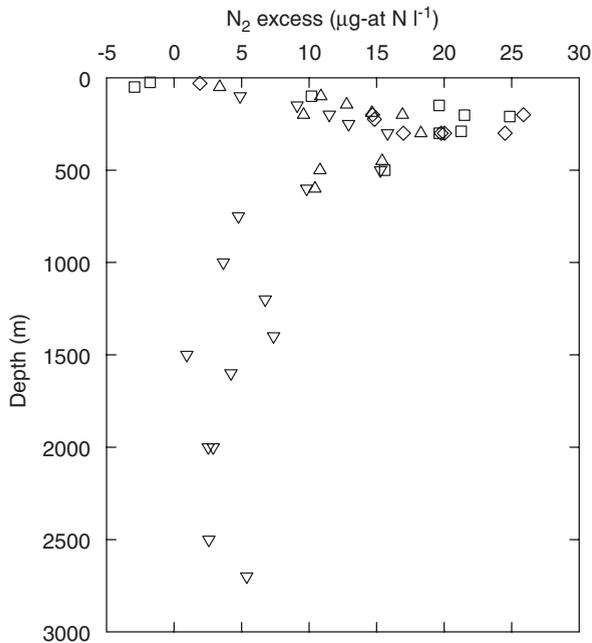
Fig. 7. N:Ar composite ensemble excess N_2 profile derived from N_2:Ar ratios, see text for details. Symbols are the same as Fig. 6.

Fig. 8. Regression of DIN ($NO_3^- + NO_2^- + NH_4^+$) against PO_4^{-3} for all USA JGOFS data with oxygen $\geqslant 65\,\mu M$ and latitudes between $9.5°$ and $11°N$.

positive even at 2000–2500 m (i.e., well below the denitrifying layer), presumably because of vertical mixing. Brandes et al. (1998) also found enriched $^{15}NO_3^-$ profiles of similar shape extending down to 2000 m in this region, supporting this hypothesis.

It is interesting to compare the excess N_2 estimates with calculated nitrate deficits. For this comparison we used a recently developed nitrate deficit equation based on the high-quality Arabian Sea JGOFS data (Codispoti et al., 2001). Their estimate is based on a Type II linear regression of PO_4^{-3} versus inorganic nitrogen ($NO_3^- + NO_2^- + NH_4^+$). The data used were restricted to the depth range 100–1500 m, excluding samples in which the dissolved O_2 concentration was less than $65\,\mu M$ (Fig. 8). The relationship derived between expected nitrate and phosphate is

$$NO_3^{exp} = 14.89(P - 0.28), \qquad (4)$$

where 14.89 is the slope of the regression in Fig. 8, P is the measured phosphate concentration, and 0.28 is the intercept on the P-axis. The nitrate deficit, NO_{3def}, is then

$$NO_{3def} = (NO_3^{exp} - N^{obs})0.86, \qquad (5)$$

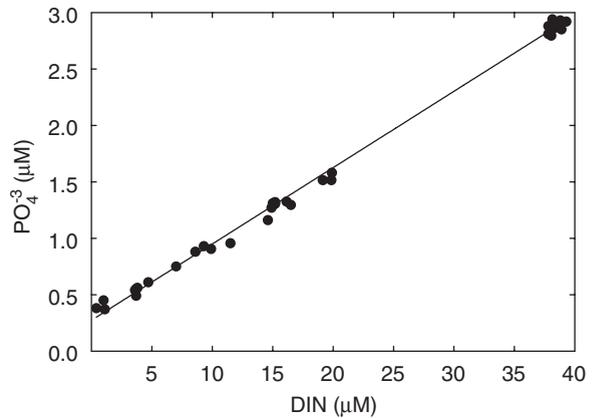where N^{obs} is the measured inorganic N ($NO_3^- + NO_2^- + NH_4^+$) and 0.86 is a factor to

account for the NH_4^+ remineralized from organic matter during denitrification (based on the assumption that the local N:P regeneration ratio is 14.89 and that during denitrification 94.4 NO_3^- are consumed for every PO_4^{-3} remineralized). This equation yields slightly higher values of NO_{3def} than most previous methods and it avoids the problems of negative deficits in the surface layer (Fig. 9). Significantly, the deficits it predicts in the water column and this distribution appear to better parallel our excess N_2 profile. The overall effect is to increase the depth-integrated nitrate deficit.

There are distinct differences between the measured N_2 excess and calculated nitrate deficit (Fig. 10). Most notably, peak values of measured N_2 excesses ($\sim$16–23 μg-at N) are much higher than the corresponding nitrate deficit ($\sim$8–10 μg-at N), with the anomaly persisting well below the depth of the nitrate deficit maximum (within the depth zone 250–600 m). Both excess N_2 and measurable nitrate deficits are present down to approximately 1500 m. We do not believe that the large excess N_2 values are an experimental artifact because all profiles from the other Indian ocean stations are similar despite the large range in dissolved oxygen (Fig. 5) and because these profiles are similar to all other profiles from other oceans. Also, there are many replicate N_2 excess measurements from four separate cruises, and there are no other likely sources for N_2 other than denitrification. Thus, we believe our measurements of excess N_2 are accurate. However, there are several possible factors that could contribute to artificially low estimates of denitrification based on nitrate deficit.
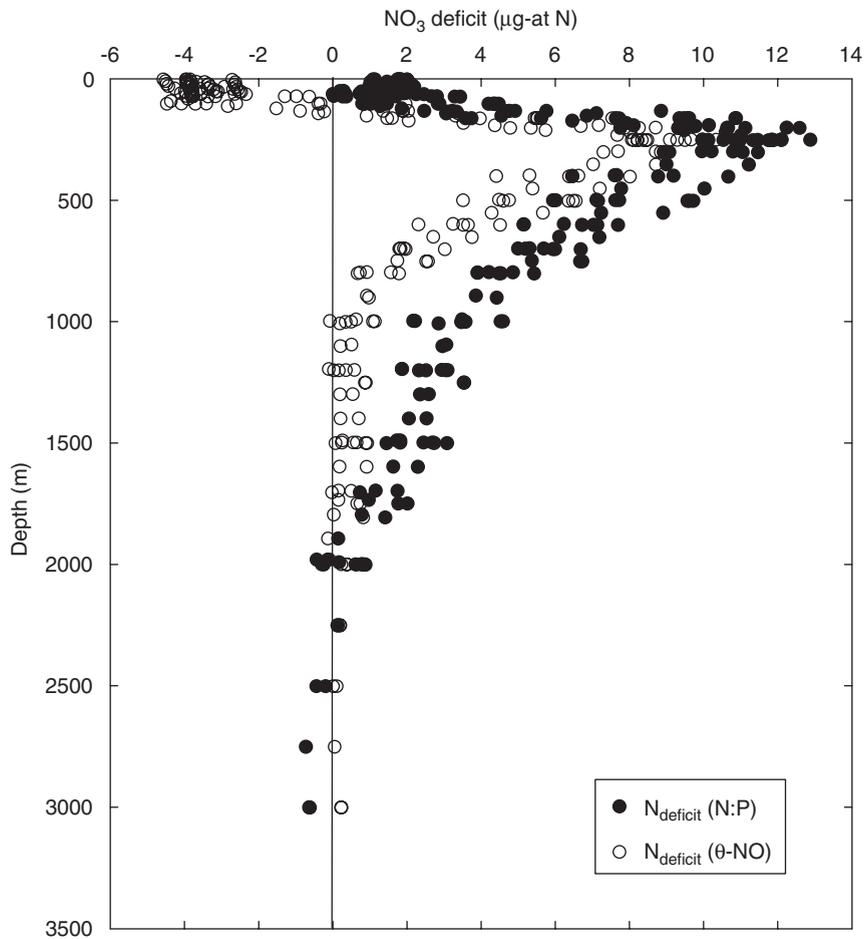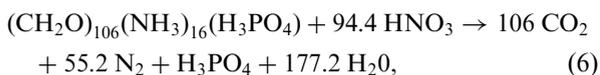
Fig. 9. Comparison of Codispoti et al. N-deficit values with typical N-deficit values calculated from a θ–NO relationship used previously in the Arabian Sea (data are from cruises TGT 043 and TGT 045 of the USA-JGOFS program).

As discussed above, nitrate deficits are not all-inclusive estimates for the total amount of N_2 produced during denitrification. The remineralization of organic amino groups and subsequent denitrification of NH_3 produced, possibly accomplished by an anammox type organism (Dalsgaard et al., 2003; Kuypers et al., 2003; Jetten et al., 2003), is a process that would not be accounted for in the nitrate-deficit calculation. Since ammonia concentrations are insignificant within the ODZ, there is reason to believe this nitrification–denitrification process is occurring.

Assuming Redfield stoichiometry we can calculate the additional contribution of N_2 from the organic N. Given by the following (Richards, 1965):

$$(CH_2O)_{106}(NH_3)_{16}(H_3PO_4) + 94.4\,HNO_3 \rightarrow 106\,CO_2$$
$$+\ 55.2\,N_2 + H_3PO_4 + 177.2\,H_2O, \qquad (6)$$

42.2 mol of N_2 are produced from the conversion of NO_3^-–N_2 (94.4/2) and 8 are derived from the oxidation of organic NH_3–N_2. Thus, if we consider the denitrification of the organic N, the N_2 produced would be higher by a factor of 55.2/47.2, which corresponds to a 16.9% increase. Although significant this is not nearly enough to account for the excess N_2 discrepancy.

Another assumption in the nitrate-deficit calculation that would lead it to be an underestimate is in the composition of the organic matter that is remineralized by NO_3^-. Recent research by Van Mooy et al. (2002) indicates that organic matter degraded during denitrification may consist primarily of proteins having a composition different from that assumed in Eq. (6). Assuming an average protein composition as given by Anderson (1995), Van Mooy et al. (2002) proposed the following
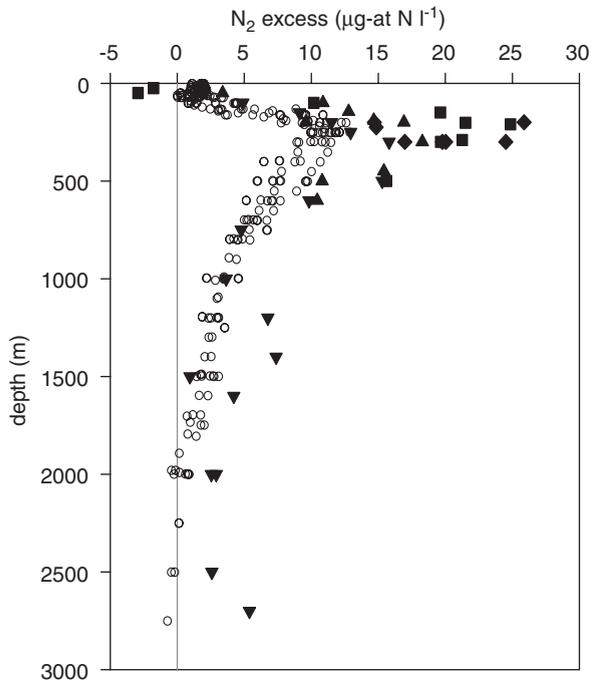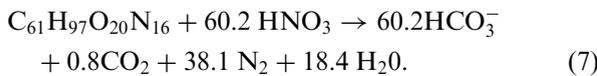
Fig. 10. Comparison of N_2-excess derived from N_2:Ar ratios (solid symbols) with the nitrate deficit derived from N:P stoichiometry by Codispoti et al., 2001 (open symbols).

stoichiometry for denitrification:

$$C_{61}H_{97}O_{20}N_{16} + 60.2\,HNO_3 \rightarrow 60.2HCO_3^- \\ + 0.8CO_2 + 38.1\,N_2 + 18.4\,H_20. \qquad (7)$$

Although Van Mooy et al. (2002) did not include *P* in their equation, if the N:P remained Redfieldian, the equation would predict an excess N_2 27% greater than Eq. (6). However, if there is preferential degradation of proteins during denitrification then the N:P remineralization ratio may well be higher. At the maximum, if there were no *P* remineralized during denitrification then Van Mooy et al. (2002) stoichiometry would yield 42% more N_2 than Eq. (6).

Significant nitrogen fixation in the Arabian Sea may also elevate N_2 yields during denitrification because *N*-fixers have N:P ratios on the order of 45 (Capone et al., 2005; Karl et al., 2002). Based on isotopic evidence, Brandes et al. (1998) estimated that 20–30% of the primary production in the Arabian Sea is fueled by nitrogen fixation. In that case, assuming the N:P ratio of organic matter produced by *N*-fixers to be 45, this, in itself, would raise the yield of N_2 during denitrification by about 50%. This would also require an increased role for anammox because the extra *N* from *N*-fixation

would be remineralized to NH_4^+ and would require anammox to convert it to N_2. Finally, in the water column there are additional reactions that could occur between Fe, Mn, I and N species that could lead to the production of N_2 (Codispoti et al., 2005; Luther et al., 1997; Farrenkopf et al., 1997).

Sedimentary processes could also contribute to the excess N_2 to the extent that they are not accompanied by an associated release of PO_4^{-3}. The most obvious of these is denitrification, but most of the nitrate converted to N_2 in the sediments would likely diffuse in from the overlying water and would already have been included in the nitrate deficit calculation. However, in sediments in contact with the ODZ the dominant sedimentary carbon remineralization reaction is sulfate reduction. In suboxic zone sediments like those in the Arabian Sea ODZ, gliding bacteria such as *Thioploca*, *Beggiatoa* and *Thiomargarita* actively transport nitrate from the overlying water into the sediments where it is used for sulfide oxidation to generate energy. However, it is thought that most of the nitrate is converted to ammonium (Jørgensen and Gallardo, 1999; Otte et al., 1999) and high ammonium fluxes have been measured from *Thioploca* mats on the Chile margin (Farrias, 1998) where a similar ODZ exists. *Thioploca* mats have also been observed in the Arabian Sea (Jørgensen and Gallardo, 1999; Levin et al., 1997) and if a similar export of NH_4^+ takes place from Arabian Sea sediments then it is likely converted to N_2 via an annamox type reaction because significant ammonium accumulation does not occur in the ODZ waters. At the extreme, if all the NH_4^+ resulting from carbon oxidation in the sediments surrounding the Arabian Sea were converted to N_2 by anammox, then the overall stoichiometry of carbon oxidation in the sediments would appear to be that of canonical denitrification, even though the main carbon oxidation pathway was sulfate reduction.

Thus, it appears that the excess N_2 in the ODZ of the Arabian Sea is significantly greater than that supportable by the estimated nitrate deficit alone. Although it is difficult to attribute this to a single process, there are several possible mechanisms to increase the N_2 yield during denitrification; these include: (1) oxidation of the ammonium regenerated during water-column denitrification to N_2, (2) denitrification fueled by non-Redfield organic matter such as preferential degradation of proteins or high N:P ratio material produced during N-fixation, (3) contributions of N_2 resulting from processes

taking place within the sediments in contact with the ODZ waters, and (4) other reactions between metals, iodine and various N species that lead to N_2 production. Because the excess N_2 values are somewhat less than double the N deficits, making the same residence time and areal extent of denitrification assumptions as used in the indirect estimates discussed above, would give denitrification rate values correspondingly greater. (Again, we are defining denitrification as the conversion of combined nitrogen to N_2 gas.)

Acknowledgments

References

Anderson, L.A., 1995. On the hydrogen and oxygen content of marine Phytoplankton. Deep-Sea Research Part I 42, 1675–1680.

Bange, H.W., Rixen, T., Johansen, A.M., Siefert, R.L., Ramesh, R., Ittekkot, V., Hoffmann, M.R., Andreae, M.O., 2000. A revised nitrogen budget for the Arabian Sea. Global Biogeochemical Cycles 14, 1283–1297.

Barber, R.T., Marra, J., Bidigare, R.C., Codispoti, L.A., Halpern, D., Johnson, Z., Latasa, M., Goericke, R., Smith, S.L., 2001. Primary productivity and its regulation in the Arabian Sea during 1995. Deep-Sea Research II 48, 1127–1172.

Brandes, J.A., Devol, A.H., Yoshinari, T., Jayakumar, D.A., Naqvi, S.W.A., 1998. Isotopic composition of nitrate in the central Arabian Sea and eastern tropical North Pacific: a tracer for mixing and nitrogen cycles. Limnology and Oceanography 43, 1680–1689.

Broecker, W.S., 1974. "NO", a conservative water-mass tracer. Earth and Planetary Science Letters 23, 100–107.

Capone, D., Burnes, J.A., Mahaffey, C.L., Gunderson, T., Michaels, T., Montoya, J.P., Subramaniam, A., Carpenter, E., 2005. Nitrogen fixation by *Trichodesmium* spp.: an important source of new nitrogen to the tropical and subtropical North Atlantic Ocean. Global Biogeochemical Cycles, 19 doi:10.1029/2004GB002331.

Codispoti, L.A., 1989. Phosphorus vs Nitrogen limitation of new and export production. In: Berger, W.H., Smetacek, V.S., Wefer, G. (Eds.), Productivity of the Oceans: Present and Past. Wiley and Sons, New York, pp. 377–394.

Codispoti, L.A., 1995. Is the ocean losing nitrate? Nature 376, 724.

Codispoti, L.A., Christensen, J.P., 1985. Nitrification, denitrification, and nitrous oxide cycling in the eastern tropical South Pacific. Marine Chemistry 16, 277–300.

Codispoti, L.A., Packard, T.T., 1980. Denitrification rates in the eastern tropical South Pacific. Journal of Marine Research 38, 453–477.

Codispoti, L.A., Brandes, J.A., Christensen, J.P., Devol, A.H., Navi, S.W.A., Pearl, H.W., Yoshinari, T., 2001. The oceanic fixed nitrogen and nitrous oxide budgets: Moving targets as we enter the anthropocene? Scientia Marina 65, 85–105.

Codispoti, L.A., Yoshinari, T., Devol, A.H., 2005. Suboxic respiration in the oceanic water-column. In: del Giorgio, P.A., Williams, P.J.l.B. (Eds.), Respiration in Aquatic Ecosystems. Oxford University Press, Oxford, pp. 225–247.

Dalsgaard, T., Thamdrup, B., 2002. Factors controlling anaerobic ammonium oxidation with nitrite in marine sediments. Applied and Environmental Microbiology 68, 3802–3808.

Dalsgaard, T., Canfield, D.E., Petersen, J., Thamdrup, B., Acuña-Gonzáles, J., 2003. N_2 production by anammox in the anoxic water column of Gulfo Dulce, Costa Rica. Nature 442.

Deutsch, C., Gruber, N., Key, R.M., Sarmiento, J.L., 2001. Dentirification and N_2 fixation in the Pacific Ocean. Global Biogeochemical Cycles 15, 483–506.

Devol, A.H., 2003. Solution to a marine mystery. Nature 422, 575–576.

Dueser, W.G., Ross, E.H., Mlodzinska, M.J., 1978. Evidence for and rate of denitrification in the Arabian Sea. Deep-Sea Research 24, 431–445.

Emerson, S., Quay, P., Stump, C., Wilbur, D., Knox, M., 1991. O_2, Ar, N_2, and ^{222}Rn in surface waters of the subarctic Pacific Ocean: net biological O_2 production. Global Biogeochemical Cycles 5, 49–69.

Emerson, S.E., Stump, C., Wilbur, D., Quay, P., 1999. Accurate measurement of O_2, N_2, and Ar gases in water and the solubility of N_2. Marine Chemistry 64, 337–347.

Farrenkopf, A.M., Dollhopf, M.E., Chadhain, S.N., Luther, G.W.I., Nealson, K.H., 1997. Reduction of iodate in seawater during Arabian Sea shipboard incubations and in laboratory cultures of the marine bacterium *Shewanella puterfaciens* strain MR-4. Marine Chemistry 57, 347–354.

Farrias, L., 1998. Potential role of bacterial mats in the nitrogen budget of marine sediments: a case of *Thioploca* sp. Marine Ecology Progress Series 170, 91–292.

Grasshoff, K., Ehrardt, M., Dremling, K., Almgran, T., 1983. Methods of Seawater Analysis. Verlag Chemie, Weinheim, (419p).

Gruber, N., Sarmiento, J., 1997. Global patterns of marine nitrogen fixation and denitrification. Global Biogeochemical Cycles 11, 235–266.

Hamme, R., 2003. Applications of neon, nitrogen and oxygen to physical, chemical and biological cycles in the ocean. Ph.D., University of Washington, 177p.

Hamme, R.C., Emerson, S.R., 2003. Mechanisms controling the global oceanic distribution of the inert gases argon, nitrogen and neon. Geophysical Research Letters 23, 35(31)–35(34).

Howell, E.A., Doney, S.C., Fine, R.A., Olson, D.B., 1997. Geochemical estimates of denitrification in the Arabian Sea and Bay of Bengal during WOCE. Geophysical Research Letters 24, 2549.

Jetten, M.S.M., Sliekers, O., Kuypers, M., Dalsgaard, T., van Niftrik, L., Cirpus, I., van de Pas-Schoonen, K., Lavik, G., Thamdrup, B., Le Paslier, D., Op den Camp, H.J.M., Hulth, S., Nielsen, L.P., Abma, W., Third, K., Engstrom, P., Kuenen, J.G., Jorgensen, B.B., Canfield, D.E., Damste, J.S.S., Revsbech, N.P., Fuerst, J., Weissenbach, J., Wagner, M., Schmidt, I., Schmid, M., Strous, M., 2003. Anaerobic ammonium oxidation by marine and freshwater planctomycete-like bacteria. Applied Microbiology and Biotechnology 63, 107–114.

Jørgensen, B.B., Gallardo, V.A., 1999. *Thioploca* spp: fillamentous sulfer bacteria with nitrate vacuoles. FEMS Microbiology Ecology 28.

Karl, D.M., Michaels, A., Bergman, B., Capone, D., Carpenter, El., Letelier, R., Paerl, H., Sigman, D., Stal, L., 2002. Dinitrogen fixation in the world's oceans. Biogeochemistry 57/58, 47–98.

Kawamiya, M., Oschlies, A., 2003. An ecosystem model for the Arabian Sea embedded into an eddy-permitting primitive-equation model: comparisons with observations. Journal of Marine Systems 38, 221–257.

Kuypers, M.M.M., Sliekers, A.O., Lavik, G., Schmid, M., Jørgensen, B.B., Kkuenen, J.G., Sinningh Damste, J.S., Strous, M., Jetten, M.S.M., 2003. Anammox planctomycetes short-cut the Black Sea nitrogen cycle. Nature 422, 606–608.

Lee, C., Murray, D.W., Barber, R.T., Buesseler, K.O., Dymond, J., Hedges, J.I., Honjo, S., Manganimi, S.J., Marra, J., Moser, C., Peterson, M.S.W.L.P., Wakeham, S.G., 1998. Particulate organic carbon fluxes: compilation of results from the 1995 US JGOFS Arabian Sea process study. Deep-Sea Research 45, 2489–2501.

Levin, L.A., Gage, J., Lamont, P., Cammidge, L., Martin, C., Patience, A., Crooks, J., 1997. Infaunal community structure in a low-oxygen, organic rich habitat on the Oman continental slope, NW Arabian Sea. In: Hawkins, L.E., Hutchinson, S. (Eds.), The Responses of Marine Organisms to their Environments. University of Southhampton, Southhampton.

Luther, G.W.I., Sundby, B., Lewis, B.L., Brendel, P.J., Silverberg, N., 1997. Interactions of manganese with the nitrogen cycle: alternative pathways to dinitrogen. Geochimica et Cosmochimica Acta 61, 4043–4054.

Mantoura, R.F.C., Law, C.S., Owens, N.P.J., Burkill, P.H., Woodward, M.S., Howland, R.J.M., Llewellyn, C.A., 1993. Nitrogen biogeochemical cycling in the northwestern Indian Ocean. Deep-Sea Research 40, 651–671.

Middelburg, J.J., Soetaert, K., Herman, P.M.J., Heip, C.H.R., 1996. Denitrification in marine sediments: a model study. Global Biogeochemical Cycles 10, 661–673.

Morrison, J.M., Codispoti, L.A., Smith, S., Wishner, K., Flagg, C., Gardner, W.E., Gaurin, S., Naqvi, S.W.A., Manghnani, V., Prosperie, L., Gundersen, J.S., 1999. The oxygen minimum zone in the Arabian Sea during 1995. Deep-Sea Research II 46, 1903–1932.

Naqvi, S.W.A., 1987. Some aspects of the oxygen-deficient conditions and denitrification in the Arabian Sea. Journal of Marine Research 45, 1049–1072.

Naqvi, S.W.A., Sen Gupta, R., 1985. "NO", a useful tool for the estimation of nitrate deficits in the Arabian Sea. Deep-Sea Research 32, 665–674.

Naqvi, S.W.A., Shailaja, M.S., 1993. Activity of the respiratory electron transport system and respiration rates within the oxygen minimum layer of the Arabian Sea. Deep-Sea Research I 40, 687–696.

Naqvi, S.W.A., Jayakumar, D.A., Narvekar, P.V., Naik, H., Sarma, V.V.S.S., D'Sousa, W., Joseph, S., George, M.D., 2000. Increased marine production of N_2O due to intensifying anoxia on the Indian Continental shelf. Nature 408, 346–349.

Naqvi, S.W.A., Niak, H., Narvekar, P.V., 2003. The Arabian Sea. In: Black, K., Scimmield, G. (Eds.), Biogeochemistry of Marine Systems. Blackwell Publishing, Oxford, pp. 157–207.

Niak, H., 2003. Benthic Nitrogen cycling with special reference to nitrous oxide in coastal and continental shelf environments of the eastern Arabian Sea. Ph.D., Goa University, p. 147.

Otte, S., Kuenen, J.G., Nielsen, L.P., Paerl, H.W., Zopfi, J., Schulz, H.N., Teske, A.S.B., Gallardo, V.A., Jørgensen, B.B., 1999. Nitrogen, carbon, and sulfur metabolism in natural *Thioploca* samples. Applied and Environmental Microbiology 65, 31348–31357.

Packard, T.T., 1971. The measurement of respiratory electron transport activity in marine phytoplankton. Journal of Marine Research 29, 235–244.

Richards, F.A., 1965. Anoxic basins and fjords. In: Riley, J.P., Skirrow, G. (Eds.), Chemical Oceanography, vol. 1. Academic Press, London and New York, pp. 611–645.

Smith, S., Roman, M., Prusova, I., Wishner, K., Gowing, M., Codispoti, L.A., Barber, R., Marra, J., Flagg, C., 1998. Seasonal response of zooplankton to monsoonal reversals in the Arabian Sea. Deep-Sea Research II 45, 2369–2403.

Swallow, J.C., 1984. Some aspects of the physical oceanography of the Indian Ocean. Deep-Sea Research 31.

Van Mooy, B.A.S., Keil, R.G., Devol, A.H., 2002. Impact of suboxia on sinking particulate organic carbon: Enhanced carbon flux and preferential degradation of amino acids via dentirification. Geochimica et Cosmochimica Acta 66, 457–465.

Warren, B.A., 1994. Context of the suboxic layer in the Arabian Sea. In: Lal, D. (Ed.), Proceedings of the Indian Academy of Sciences. Lotus Printers, New Delhi, pp. 203–216.

Yakushev, E.V., Neretin, L.N., 1997. One-dimensional modeling of nitrogen and sulfur cycles in the aphotic zones of the Black and Arabian Seas. Global Biogeochemical Cycles 11, 401–414.